

Vibrational Circular Dichroism of Africanane and Lippifoliane Sesquiterpenes from *Lippia integrifolia*

Carlos M. Cerda-García-Rojas,^{*,†} César A. N. Catalán,[‡] Ana C. Muro,[‡] and Pedro Joseph-Nathan[†]

Departamento de Química, Centro de Investigación y de Estudios Avanzados del Instituto Politécnico Nacional, Apartado 14-740, México, D. F., 07000 México, and Instituto de Química Orgánica, Facultad de Bioquímica, Química y Farmacia, Universidad Nacional de Tucumán, Ayacucho 471, S. M. de Tucumán, T4000INI Argentina

Received February 9, 2008

The agreement between theoretical and experimental vibrational circular dichroism curves of (4*R*,9*R*,10*R*)-(+)-african-1(5)-ene-2,6-dione (**1**) and (4*R*,9*S*,10*R*)-lippifoli-1(6)-en-5-one (**2**), isolated from the widely used plant *Lippia integrifolia*, allowed the determination of the conformation and absolute configuration of **1** and confirmed both structural features for **2**. Molecular modeling of **1** and **2** was carried out by means of a systematic and a Monte Carlo search protocol followed by geometry optimization employing density functional theory calculations with the B3LYP/6-31G(d), B3LYP/DGDZVP, and/or B3PW91/DGDZVP2 functionals/basis sets. Validation of the minimum energy conformations for both tricyclic substances was achieved by comparison of the experimental and theoretical vicinal ¹H–¹H NMR coupling constants obtained by DFT-GIAO calculations.

Lippia integrifolia Hieron. (Verbenaceae), a woody aromatic shrub native to central and northern Argentina, is widely used in a large number of commercial preparations and in traditional medicine as a diuretic, emmenagogue, stomachic, and nervine agent.^{1,2} This plant produces a series of secondary metabolites that includes africananes,^{2,3} e.g., **1**, derived from the tricyclo[6.3.0.0^{2,4}]undecane ring system, and lippifolianes,⁴ e.g., **2** and **3**, containing the tricyclo[5.4.0.0^{2,4}]undecane moiety (Figure 1). In a previous study,⁵ the absolute configuration of lippifolianes was assigned by analysis of the electronic circular dichroism data in combination with density functional theory minimum energy molecular models of (4*R*,9*S*,10*R*)-lippifoli-1(6)-en-5-one (**2**), (1*S*,4*R*,6*S*,9*S*,10*R*)-lippifolien-1-ol-5-one (**3**), and (4*S*,9*S*,10*R*)-lippifoli-1(6)-en-4-ol-5-one (**4**) and application of the octant rule for saturated ketone **3** and the helicity rules for α,β -unsaturated ketones **2** and **4**. The results were corroborated by the anomalous dispersion effect observed in the X-ray diffraction analysis of (4*S*,9*S*,10*R*)-4,10,11-tribromo-10,11-*seco*-lippifoli-1(6)-en-5-one (**5**) prepared from **2**. In the same work,⁵ the absolute configuration of africanane derivatives as **1** was proposed on the basis of biogenetic relationships among the natural products isolated from *L. integrifolia*, since the biogenesis of africananes was considered as structurally interrelated with the biogenesis of lippifolianes.⁵ Africanane derivatives have been isolated from diverse natural sources also including the liverworts *Pellia epiphylla*,⁶ *Porella caespitans*,⁷ and *Porella swartziana*,⁸ the ascomycete *Leptographium lundbergii*,⁹ and the soft coral *Simularia dissecta*.¹⁰

The absolute configuration of africanane derivatives from *L. integrifolia* can be strongly supported if a selected representative compound of this kind is studied by vibrational circular dichroism (VCD) spectroscopy.^{11–15} This technique, which has been recently used to determine the absolute configuration of several natural products,^{16–27} is based on comparison between the experimental VCD spectrum and the corresponding theoretical curve for the proper enantiomer obtained by density functional theory (DFT)²⁸ calculations of the vibrational frequencies and VCD intensities. The calculations involve generation of weighted-averaged vibrational plots including all significantly populated conformations of the analyzed molecule. In this study, africanane derivative **1** was

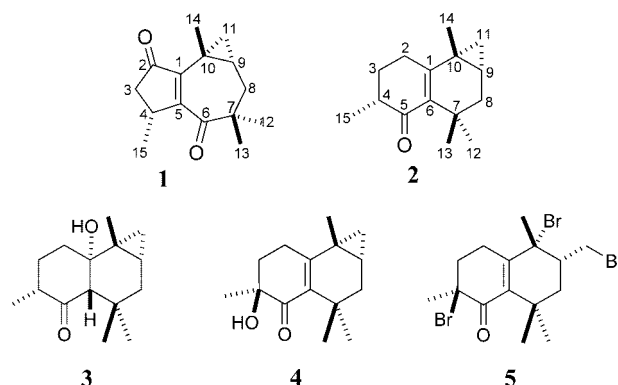


Figure 1. Africanane **1**, lippifolianes **2–4**, and *seco*-lippifoliane **5** derivatives.

selected because it contains an interestingly functionalized tricyclic system and only one predominant conformation. On the other hand, lippifoliane **2**, whose absolute configuration was securely solved by X-ray diffraction analysis of the brominated derivative **5**,⁵ was also studied herein by applying the VCD methodology. Lippifoliane **2**, which exhibits four conformations, was used as a reference compound to provide certainty in the VCD calculations.

Results and Discussion

(4*R*,9*R*,10*R*)-(+)-African-1(5)-ene-2,6-dione (**1**) and (4*R*,9*S*,10*R*)-lippifoli-1(6)-en-5-one (**2**) were obtained from the essential oil of *L. integrifolia* as previously described.^{2,4} The experimental VCD spectra of **1** and **2**, measured from CCl₄ solutions, are depicted in Figures 2a and 3a, respectively. On the other hand, the series of theoretical VCD spectra for these substances were obtained employing a molecular modeling protocol, which initially involved the use of systematic and Monte Carlo conformational searching methods.²⁹ The molecular models of **1** and **2** were constructed starting from minimized [5.3.0] and [4.4.0] bicyclic systems, respectively, followed by consecutive incorporation of the three-membered ring, the carbonyl, and methyl groups. In each step, a full minimization routine employing the MMFF94 molecular mechanics force field³⁰ was carried out. In this process the energy value was monitored as a convergence criterion to yield the global minimum energy structures. The Monte Carlo search using the global minimum of **1** and **2** as the starting point afforded two

* To whom correspondence should be addressed. Tel: (+52-55)-5747-7112. Fax: (+52-55)-5747-7137. E-mail: ccerda@cinvestav.mx.

[†] Centro de Investigación y de Estudios Avanzados del Instituto Politécnico Nacional, México, D. F.

[‡] Universidad Nacional de Tucumán.

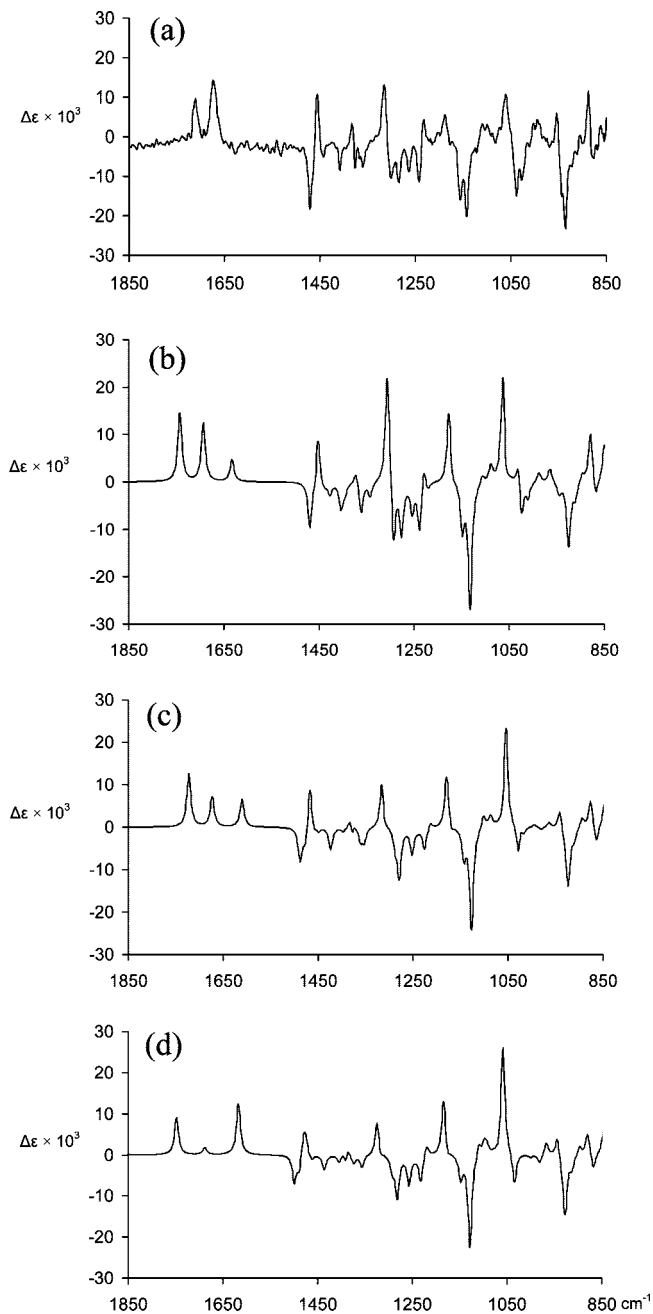


Figure 2. Experimental (a) and DFT-calculated (b) B3PW91/DGDZVP2, (c) B3LYP/DGDZVP, and (d) B3LYP/6-31G(d) VCD spectra of **1**.

conformers for **1** of $E_{\text{MMFF}} = 38.942$ and 47.942 kcal/mol and four conformers for **2** of $E_{\text{MMFF}} = 41.901$, 43.868 , 45.508 , and 47.795 kcal/mol. The structures were submitted to geometry optimization using DFT calculations at the B3LYP/6-31G(d)³¹ and B3LYP/DGDZVP³² levels of theory to obtain two sets of molecular models of increasing accuracy for both sesquiterpenes. After structure optimization, the vibrational frequencies and IR and VCD intensities were calculated at the same level of theory, as well as the thermochemical parameters at 298 K and 1 atm.

On the other hand, the unambiguous conformational definition of a molecule and the contribution of each conformational species are critical points for the achievement of reliable results in the VCD technique. For this purpose, the thermochemical parameters were employed for estimation of the population of each structure in the conformational equilibrium. The relative populations were calculated according to the $\Delta G = \Delta H - T\Delta S$ and $\Delta G = -RT \ln K$ equations, considering the B3LYP/DGDZVP frequencies at 298 K

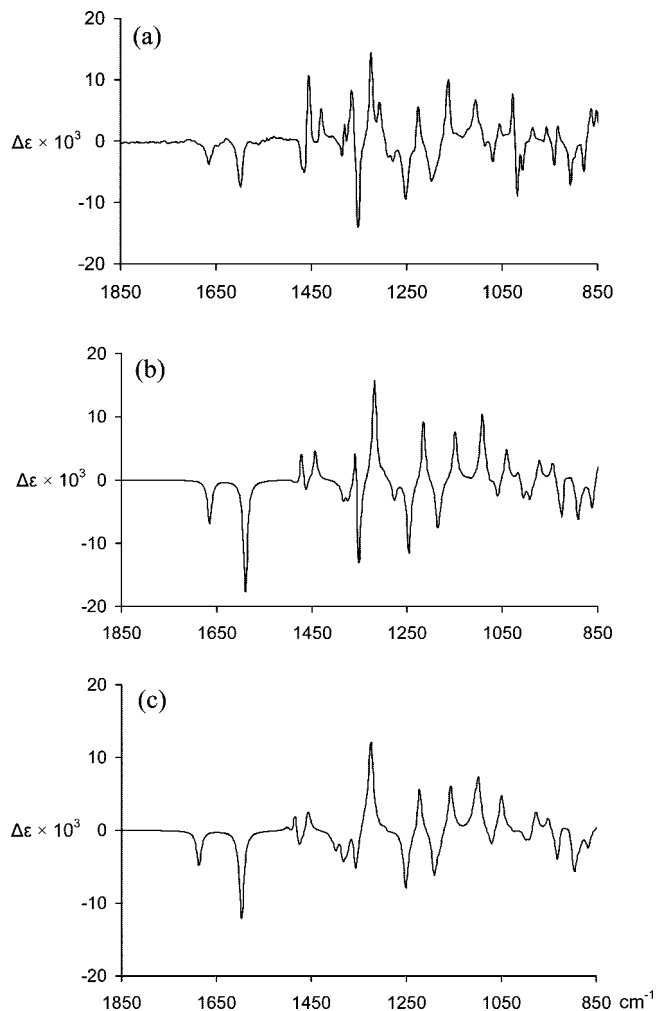


Figure 3. Experimental (a) and Boltzmann-weighted DFT-calculated (b) B3LYP/DGDZVP and (c) B3LYP/6-31G(d) VCD spectra of **2**.

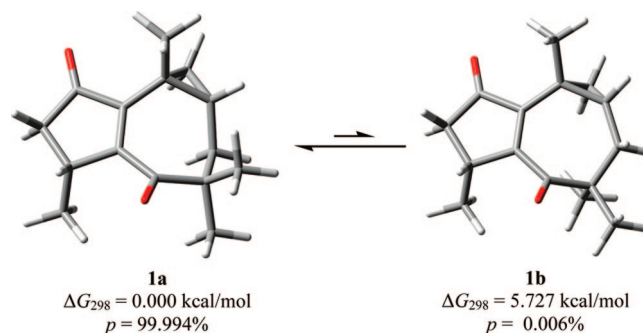


Figure 4. DFT B3LYP/DGDZVP geometry optimized conformers **1a** and **1b** at 298 K and 1 atm.

and 1 atm. Also, equations $K_{1,2} = n_2/n_1$ and $n_1 + n_2 = 1$ were considered for **1** and $K_{1,2} = n_2/n_1$, $K_{2,3} = n_3/n_2$, $K_{3,4} = n_4/n_3$, $K_{4,1} = n_1/n_4$, and $n_1 + n_2 + n_3 + n_4 = 1$ were taken into account for the equilibrium of **2**. In these equations, K_{ij} stands for equilibrium constants and n_i stands for the number of moles. The difference between the two conformations of africanane **1** resided in the seven-membered ring geometry. In conformer **1a**, whose absolute values are $E_0 = -733.818944$ au, $H_{298} = -733.801221$ au, and $G_{298} = -733.862243$ au, the C-8 atom points out toward the *endo*-face of the molecule, while in conformer **1b** this atom lies on the *exo*-face of the structure (Figure 4). According to the thermochemical analysis, the population of conformer **1b** was smaller than 0.006%,

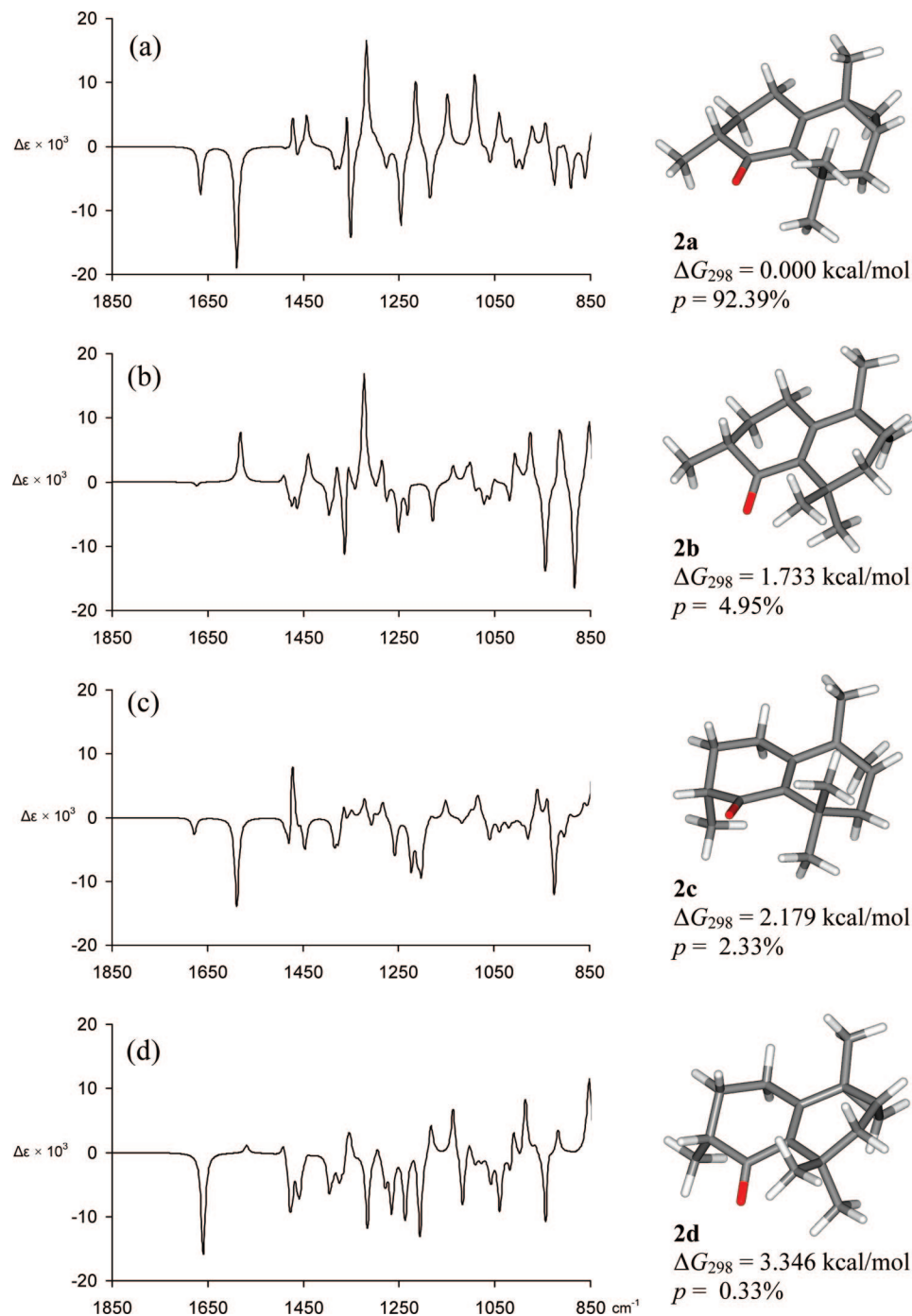


Figure 5. VCD spectra of conformers **2a–2d** calculated at the DFT B3LYP/DGDZVP level of theory at 298 K and 1 atm.

having a $\Delta G_{298} = 5.727$ kcal/mol with respect to conformer **1a**. Therefore, the contribution of conformer **1b** was neglected and structure **1a** was taken into account as the only relevant component present in africanane **1**.

Concerning lippifoliane **2**, the population analysis showed that structures **2a–2d** contribute to the conformational equilibrium with predominance of **2a** at 92.39% followed by **2b–2d** at 4.95%, 2.33%, and 0.33%, respectively (Figure 5a–d). In the global minimum structure **2a**, whose absolute values are $E_0 = -659.769680$, $H_{298} = -659.752871$, and $G_{298} = -659.811225$ au, the C-8 atom points out toward the *endo*-face of the molecule and the cyclohexenone ring, designated as ring A, adopts a half-chair conformation with the methyl group at C-4 in an equatorial position. In the second energy-minimum structure, **2b**, the methyl group at C-4 remains in an equatorial position, but there is a conformational change in ring B that moves the C-8 atoms toward the *exo*-face of the

structure. In conformers **2c** and **2d**, the half-chair conformation of ring A is inverted with respect to **2a** and **2b** with the consequent change of the methyl group toward the axial orientation. A previous conformational analysis of the lippifoliane derivative was carried out, but without consideration of the thermochemical parameters.⁵

Since the X-ray structure of lippifoliane derivative **2** was published recently,⁵ it was desirable to compare its X-ray dihedral angles with those obtained from DFT analysis. The close correspondence between the solid state dihedral angles of **2** and those of the global minimum structure **2a** supports the conformational analysis of lippifoliane derivative **2** (see Supporting Information). In the case of africanane **1**, no X-ray crystallographic data have been reported since the compound was always obtained as a colorless oil. However, the conformation can be supported experimentally by comparison of the experimental and theoretical vicinal ¹H NMR coupling constant values since they are highly sensitive

Table 1. DFT B3LYP/DGDZVP Calculated and Experimental NMR Coupling Constants for Africanane (**1**) and Lippifoliane (**2**)

<i>J</i>	1 ^a	1 ^b	2a ^a	2b ^a	2c ^a	2d ^a	2 _{wgt} ^c	2 ^b
2 α ,2 β			-20.0	-21.1	-21.5	-21.9	-20.1	-17.6
2 α ,3 α			4.1	5.7	5.9	5.1	4.2	4.8
2 α ,3 β			2.4	1.5	12.4	12.7	2.6	3.3
2 β ,3 α			12.9	12.0	1.3	2.1	12.5	11.4
2 β ,3 β			4.4	5.9	6.6	5.5	4.5	4.8
3 α ,3 β	-19.0	-21.4	-14.5	-14.7	-15.4	-15.1	-14.5	-13.0
3 α ,4	2.3	1.4	13.3	14.4	1.9	1.5	13.0	12.8
3 β ,4	6.7	6.3	5.2	4.5	5.4	5.8	5.2	4.8
8 α ,8 β	-14.8	-16.2	-16.6	-16.1	-16.5	-16.0	-16.6	-14.0
8 α ,9	10.9	10.0	5.3	1.7	5.3	2.1	5.1	5.8
8 β ,9	5.2	5.3	9.5	4.8	9.6	4.1	9.3	8.2
9,11 α	4.5	3.9	3.4	5.2	3.6	5.4	3.5	4.0
9,11 β	8.0	8.0	8.1	9.1	8.2	9.0	8.2	8.0
11 α ,11 β	-4.7	-6.1	-4.1	-4.4	-4.1	-4.4	-4.1	-4.0

^a Calculated with the GIAO method using the B3LYP/DGDZVP-optimized structures. ^b Measured from CDCl₃ solutions at 300 MHz. ^c Boltzmann-weighted average of **2a**–**2d** according to the DFT population.

to geometry. The theoretical ³J_{HH} coupling constants were calculated using the gauge-including atomic orbitals (GIAO) method³³ at the B3LYP/DGDZVP level, affording the values listed in Table 1. Although in several works the coupling constant values of natural products^{5,24,34,35} were calculated from DFT dihedral angles through an empirically parametrized equation,^{36,37} application of the DFT-GIAO method for the calculation of coupling constants in natural compounds is a relatively new issue. One example for a biologically relevant molecule has been explored in detail recently.³⁸ For lippifoliane conformers **2a**–**2d**, the coupling constants were calculated using the same method. Each value was Boltzmann-weighted taking into account the DFT population listed in Figure 5a–d to integrate the population-weighted average coupling constants for **2**. The good correlation between the two sets of NMR parameters indicated that the conformations and populations of lippifoliane **2** in solution are quite similar to those found in the DFT molecular models.

Once the conformational analysis of **1** and **2** was secured, the theoretical VCD spectra were generated scaling the vibrational frequencies with an anharmonicity factor of 0.97. In all vibrational plots, band shapes are Lorentzian and bandwidths are 6 cm⁻¹. For africanane **1**, which remains in only one highly predominant conformer (**1a**), we employed the B3LYP/6-31G(d) and B3LYP/DGDZVP levels of theory (Figure 2, parts d and c, respectively) but also included one additional calculation at a higher level using the B3PW91/DGDZVP2 basis set (Figure 2b). This last calculation improved the carbonyl stretching region of the spectrum, which has been shown as a difficult region to obtain reliable spectra due to the presence of artifacts.^{23b} For lippifoliane **2**, individual spectra were obtained for each conformer **2a**–**2d** to afford four plots for every basis set. Those corresponding to the B3LYP/DGDZVP level of theory are depicted in Figure 5a–d. It is interesting to point out the dramatic change in intensity and phase observed for the stretching band of the C=C group along the four conformers (Figure 5a–d). This variation justifies the accurate estimation of the conformational population when VCD spectroscopy is used. The four plots were combined according to the molar fraction of each conformational species to provide the Boltzmann-weighted-averaged spectra depicted in Figure 3b. The same procedure was applied to the VCD frequencies arising from the B3LYP/6-31G(d) calculations, whose final plot is depicted in Figure 3c. The B3LYP/6-31G(d) level of theory has been used in several studies, affording reliable enough results to unambiguously establish the absolute configuration of organic compounds.^{12,13} In addition we included calculations at the B3LYP/DGDZVP level, which turned out to be more accurate (Figure 3) and of faster performance than B3LYP/6-31G(d) calculations, because the DGauss basis sets such as DGDZVP are optimized for DFT methods.³²

In summary, comparison between the experimental and calculated VCD spectra showed good agreement (Figures 2 and 3) and clearly

established that (+)-african-1(5)-ene-2,6-dione (**1**) has the (4*R*, 9*R*, 10*R*) absolute configuration, coincident with that previously proposed on the basis of its biogenetic relationship with lippifolianes,⁵ while lippifoli-1(6)-en-5-one (**2**) certainly corresponds to the (4*R*, 9*S*, 10*R*) enantiomer, as previously found by X-ray diffraction analysis of **5**.⁵

It can be concluded that VCD spectroscopy can be efficiently applied to secure the absolute configuration of lippifolianes and africananes. Full certainty about the absolute configuration of natural products allows the delineation of biogenetic and evolutive relationships among diverse organisms that contain related secondary metabolites. The absolute configuration of africanane derivatives isolated from *L. integrifolia* (Verbenaceae) is the same as that of africananes isolated from *Pellia epiphylla*,³ *Porella caespitans*,⁷ and *P. swartziana*⁸ (Hepaticae), which suggests that africanane derivatives from higher plants and liverworts could have a similar biogenetic origin. Concerning the absolute configuration of africananes isolated from other species, such as the fungus *Lep- tographium lundbergii*⁹ and the soft coral *Simularia dissecta*,¹⁰ no studies have been yet carried out, although it would be desirable to explore if the absolute configuration of these africanane derivatives varies according to their origin in nature.

Experimental Section

General Experimental Procedures. VCD and IR measurements were performed on a dualPEM Chiral/IR FT-VCD spectrophotometer at BioTools, Inc. (Jupiter, FL). Samples of **1** (5.0 mg) and **2** (5.2 mg) were dissolved in CCl₄ (100 μ L) and placed in a BaF₂ cell with a path length of 100 μ m. In each case, data were acquired at a resolution of 4 cm⁻¹ during 6 h.

Molecular Modeling. Geometry optimizations for **1** and **2** were carried out using the MMFF94 force-field calculations as implemented in the Spartan'04 program. The systematic conformational search for the tricyclic structures was achieved with the aid of Dreiding models considering the two extreme conformations for the five- and seven-membered rings of **1** and for the two six-membered ring of **2**, affording four combinations in each case. The *E*_{MMFF} values were used as the convergence criterion, and a further search with the Monte Carlo protocol was carried out considering an energy cutoff of 10 kcal/mol. Only two energy-minimum structures were found for **1** and four for **2**. They were optimized by DFT²² at the B3LYP/6-31G(d), B3LYP/DGDZVP, and B3PW91/DGDZVP2 levels of theory for **1** and B3LYP/6-31G(d) and B3LYP/DGDZVP levels of theory for **2** using the Gaussian 03W program. The minimized structures were used to calculate the thermochemical parameters and the IR and VCD frequencies at 298 K and 1 atm. Experimental and calculated rotational strengths (integrated VCD intensities) were obtained using the Resolutions software version 4.1.0.101 from Varian. To integrate the negative bands, the VCD intensities were multiplied by -1. ¹H–¹H vicinal coupling constants were calculated with the GIAO method as implemented in the Gaussian 03W program using the B3LYP/DGDZVP-optimized structures and the SpinSpin option³⁹ during the NMR job.

Acknowledgment. The authors thank CONACYT-Mexico for partial financial support. Work in Tucumán was supported by grants from Consejo Nacional de Investigaciones Científicas y Técnicas de Argentina (CONICET-PIP 5176/04) and Agencia Nacional de Promoción Científica y Tecnológica-Universidad Nacional de Tucumán (PICTO 2004, No. 503). Helpful support from CYTED, Spain, is also acknowledged.

Supporting Information Available: DFT-calculated atomic Cartesian coordinates for each conformer of **1** and **2** (Tables S1–S6). Comparison of X-ray and DFT B3LYP/DGDZVP dihedral angles for the rings of lippifoliolane derivative **2** (Table S7). Experimental and DFT IR spectra of **1** and **2** (Figures S1 and S2). Theoretical versus experimental integrated VCD intensity plots for **1** and **2** (Figures S3 and S4). This material is available free of charge via the Internet at <http://pubs.acs.org>.

References and Notes

- (1) Toursarkissian, M. *Plantas Medicinales de la Argentina*; Hemisferio Sur: Buenos Aires, 1980; p 135.
- (2) Catalán, C. A. N.; de Lampasona, M. E. P.; Cerda-García-Rojas, C. M.; Joseph-Nathan, P. *J. Nat. Prod.* **1995**, *58*, 1713–1717.
- (3) Fricke, C.; Hardt, I. H.; König, W. A.; Joulain, D.; Zygadlo, J. A.; Guzmán, C. A. *J. Nat. Prod.* **1999**, *62*, 694–696.
- (4) (a) Catalán, C. A. N.; de Fenik, I. J. S.; Dartayet, G. H.; Gros, E. G. *Phytochemistry* **1991**, *30*, 1323–1326. (b) Catalán, C. A. N.; de Lampasona, M. E. P.; de Fenik, I. J. S.; Cerda-García-Rojas, C. M.; Mora-Pérez, Y.; Joseph-Nathan, P. *J. Nat. Prod.* **1994**, *57*, 206–210.
- (5) Cerda-García-Rojas, C. M.; Coronel, A. C.; de Lampasona, M. E. P.; Catalán, C. A. N.; Joseph-Nathan, P. *J. Nat. Prod.* **2005**, *68*, 659–665.
- (6) Cullmann, F.; Becker, H. *Phytochemistry* **1998**, *47*, 237–245.
- (7) Toyota, M.; Nagashima, F.; Shima, K.; Asakawa, Y. *Phytochemistry* **1992**, *31*, 183–189.
- (8) Tori, M.; Nakashima, K.; Takeda, T.; Kan, Y.; Takaoka, S.; Asakawa, Y. *Tetrahedron* **1996**, *52*, 6339–6354.
- (9) Abraham, W. R.; Ernst, L.; Witte, L.; Hanssen, H. P.; Sprecher, E. *Tetrahedron* **1986**, *42*, 4475–4480.
- (10) Ramesh, P.; Reddy, N. S.; Rao, T. P.; Venkateswarlu, Y. *J. Nat. Prod.* **1999**, *62*, 1019–1021.
- (11) Cerè, V.; Peri, F.; Pollicino, S.; Ricci, A.; Devlin, F. J.; Stephens, P. J.; Gasparrini, F.; Rompietti, R.; Villani, C. *J. Org. Chem.* **2005**, *70*, 664–669.
- (12) Kuppens, T.; Vandyck, K.; Van der Eycken, J.; Herrebout, W.; van der Veken, B. J.; Bultinck, P. *J. Org. Chem.* **2005**, *70*, 9103–9114.
- (13) (a) Freedman, T. B.; Cao, X.; Dukor, R. K.; Nafie, L. A. *Chirality* **2003**, *15*, 743–758. (b) Nafie, L. A. *Nat. Prod. Commun.* **2008**, *3*, 451–466.
- (14) Bouř, P.; Navrátilová, H.; Setnička, V.; Urbanová, M.; Volka, K. *J. Org. Chem.* **2002**, *67*, 161–168.
- (15) Wang, F.; Wang, H.; Polavarapu, P. L.; Rizzo, C. J. *J. Org. Chem.* **2001**, *66*, 3507–3512.
- (16) Lassen, P. R.; Skytte, D. M.; Hemmingsen, L.; Nielsen, S. F.; Freedman, T. B.; Nafie, L. A.; Christensen, S. B. *J. Nat. Prod.* **2005**, *68*, 1603–1609.
- (17) (a) Monde, K.; Taniguchi, T.; Miura, N.; Nishimura, S.-I.; Harada, N.; Dukor, R. K.; Nafie, L. A. *Tetrahedron Lett.* **2003**, *44*, 6017–6020. (b) Monde, K.; Taniguchi, T.; Miura, N.; Kutschy, P.; Čurillová, Z.; Pilátová, M.; Mojžiš, J. *Bioorg. Med. Chem.* **2005**, *13*, 5206–5212. (c) Monde, K.; Taniguchi, T.; Miura, N.; Vairappan, C. S.; Suzuki, M. *Tetrahedron Lett.* **2006**, *47*, 4389–4392. (d) Monde, K.; Taniguchi, T.; Miura, N.; Vairappan, C. S.; Suzuki, M. *Chirality* **2006**, *18*, 335–339.
- (18) Cichewicz, R. H.; Clifford, L. J.; Lassen, P. R.; Cao, X.; Freedman, T. B.; Nafie, L. A.; Deschamps, J. D.; Kenyon, V. A.; Flanary, J. R.; Holman, T. R.; Crews, P. *Bioorg. Med. Chem.* **2005**, *13*, 5600–5612.
- (19) Mugishima, T.; Tsuda, M.; Kasai, Y.; Ishiyama, H.; Fukushi, E.; Kawabata, J.; Watanabe, M.; Akao, K.; Kobayashi, J. *J. Org. Chem.* **2005**, *70*, 9430–9435.
- (20) Stephens, P. J.; McCann, D. M.; Devlin, F. J.; Smith, A. B., III *J. Nat. Prod.* **2006**, *69*, 1055–1064.
- (21) Muñoz, M. A.; Muñoz, O.; Joseph-Nathan, P. *J. Nat. Prod.* **2006**, *69*, 1335–1340.
- (22) Bercion, S.; Buffeteau, T.; Lespade, L.; Coupe deK. Martin, M.-A. *J. Mol. Struct.* **2006**, *791*, 186–192.
- (23) (a) Stephens, P. J.; Pan, J. J.; Devlin, F. J.; Urbanova, M.; Hajicek, J. *J. Org. Chem.* **2007**, *72*, 2508–2524. (b) Stephens, P. J.; Pan, J. J.; Devlin, F. J.; Krohn, K.; Kurtan, T. *J. Org. Chem.* **2007**, *72*, 3521–3536. (c) Stephens, P. J.; Pan, J. J.; Krohn, K. *J. Org. Chem.* **2007**, *72*, 7641–7649.
- (24) Cerda-García-Rojas, C. M.; García-Gutiérrez, H. A.; Hernández-Hernández, J. D.; Román-Marín, L. U.; Joseph-Nathan, P. *J. Nat. Prod.* **2007**, *70*, 1167–1172.
- (25) Krohn, K.; Gehle, D.; Dey, S. K.; Nahar, N.; Mosihuzzaman, M.; Sultana, N.; Sohrab, M. H.; Stephens, P. J.; Pan, J. J.; Sasse, F. *J. Nat. Prod.* **2007**, *70*, 1339–1343.
- (26) Krautmann, M.; de Riscalca, E. C.; Burgueño-Tapia, E.; Mora-Pérez, Y.; Catalán, C. A. N.; Joseph-Nathan, P. *J. Nat. Prod.* **2007**, *70*, 1173–1179.
- (27) Min, H. M.; Aye, M.; Taniguchi, T.; Miura, N.; Monde, K.; Ohzawa, K.; Nikai, T.; Niwa, M.; Takaya, Y. *Tetrahedron Lett.* **2007**, *48*, 6155–6158.
- (28) Perdew, J. P. *Phys. Rev. B* **1986**, *33*, 8822–8824.
- (29) Chang, G.; Guida, W. C.; Still, W. C. *J. Am. Chem. Soc.* **1989**, *111*, 4379–4386.
- (30) (a) Halgren, T. J. *Comput. Chem.* **1996**, *17*, 490–519. (b) Halgren, T. J. *Comput. Chem.* **1996**, *17*, 520–552. (c) Halgren, T. J. *Comput. Chem.* **1996**, *17*, 553–586. (d) Halgren, T.; Nachbar, R. B. *Comput. Chem.* **1996**, *17*, 587–615. (e) Halgren, T. J. *Comput. Chem.* **1996**, *17*, 616–641.
- (31) Hehre, W. J.; Radom, L.; Schleyer, P. v. R.; Pople, J. A. *Ab Initio Molecular Orbital Theory*; Wiley: New York, 1986.
- (32) (a) Godbout, N.; Salahub, D. R.; Andzelm, J.; Wimmer, E. *Can. J. Chem.* **1992**, *70*, 560–571. (b) Andzelm, J.; Wimmer, E. *J. Chem. Phys.* **1992**, *96*, 1280–1303.
- (33) Wolinski, K.; Hilton, J. F.; Pulay, P. *J. Am. Chem. Soc.* **1990**, *112*, 8251–8260.
- (34) Hernández-Hernández, J. D.; Román-Marín, L. U.; Cerda-García-Rojas, C. M.; Joseph-Nathan, P. *J. Nat. Prod.* **2005**, *68*, 1598–1602.
- (35) García-Granados, A.; López, P. E.; Melguizo, E.; Moliz, J. N.; Parra, A.; Simeó, Y.; Dobado, J. A. *J. Org. Chem.* **2003**, *68*, 4833–4844.
- (36) Haasnoot, C. A. G.; de Leeuw, F. A. A. M.; Altona, C. *Tetrahedron* **1980**, *36*, 2783–2792.
- (37) Cerda-García-Rojas, C. M.; Zepeda, L. G.; Joseph-Nathan, P. *Tetrahedron Comp. Methodol.* **1990**, *3*, 113–118.
- (38) Allouche, A. R.; Aubert-Frécon, M.; Graveron-Demilly, D. *Phys. Chem. Chem. Phys.* **2007**, *9*, 3098–3103.
- (39) (a) Sychrovsky, V.; Grafenstein, J.; Cremer, D. *J. Chem. Phys.* **2000**, *113*, 3530–3547. (b) Helgaker, T.; Watson, M.; Handy, N. C. *J. Chem. Phys.* **2000**, *113*, 9402–9409.

NP8000927